^{111}In-DTPA-D-Phe^{1}-Octreotide Binding and Somatostatin Receptor Subtypes in Thyroid Tumors

Eva B. Forssell-Aronsson, Ola Nilsson, Sven Anders Benjegård, Lars Kölby, Peter Bernhardt, Johan Mölne, S. Hossein Hashemi, Bo Wängberg, Lars-Erik Tisell, and Håkan Ahlman

Departments of Radiation Physics, Pathology, and Surgery, Sahlgrenska University Hospital, Göteborg University, Göteborg, Sweden

The purpose of this study was to evaluate the potential for therapy of thyroid tumors using the radiolabeled somatostatin (SS) analog octreotide. **Methods:** Concentrations of ^{111}In activity in human thyroid tumors and normal thyroid tissue and blood samples were determined 1–15 d after intravenous injection of ^{111}In-diethylenetriaminepentaacetic acid-Phe^{1}-octreotide. The results were compared with SS receptor (*sstr*) subtype profile (by Northern blot analysis) and the relative expression of the second subtype, *sstr2* (by ribonuclease protection assay, RPA). The true tumor volumes in lymph node metastases from 1 patient were estimated. In total, tissues from 68 patients were included in the study. **Results:** The highest tumor-to-blood ratio (T/B) for medullary thyroid carcinoma (MTC) was 360; for follicular adenoma (FA), 190; for Hürthle cell adenoma (HCA), 140; and for Hürthle cell carcinoma (HCC) and papillary carcinoma (PC), 70. The corresponding value was 7–18 for normal thyroid tissue, with higher values for colloid goiter (8–48) and thyroiditis (7–120). A high T/B was related to a large fraction of tumor cells in lymph node metastases. T/Bs were higher for the tumor samples with expression of *sstr2* at Northern blot analysis than for those without. All thyroid tumor types regularly expressed *sstr1*, *sstr3*, *sstr4*, and *sstr5*. *sstr2* was expressed in most MTC tumors but was not detected in FA or PC and was irregularly expressed in HCA and HCC. However, RPA analysis detected *sstr2* in all tumors studied. **Conclusion:** Despite the lack of *sstr2* at Northern blot analysis in most of the thyroid tumors studied, high T/Bs were in general found when compared with corresponding values for normal thyroid tissue. The sometimes extremely high ratios are promising and indicate a possibility of using radiolabeled octreotide for radiation therapy of *sstr*-positive tumors in the future.

Key Words: octreotide; ^{111}In; thyroid tumors; somatostatin receptors

J Nucl Med 2000; 41:636–642

Thyroid cancer is uncommon, being responsible for approximately 1% of all malignant tumors, and most cases occur in individuals between 25 and 65 y old (*1*). Tumors derived from thyroid follicular cells are follicular adenoma (FA), follicular carcinoma (FC), papillary carcinoma (PC), and anaplastic carcinoma (AC). Hürthle cell adenoma (HCA) and carcinoma (HCC) are subtypes of the follicular tumors and have oncocytic features. In contrast, medullary thyroid carcinoma (MTC) is derived from the neuroendocrine calcitonin-producing C cells. The main therapy for thyroid tumors is surgical removal. Residual tumor and metastases of FC and PC are often treated with radioiodine ($^{131}I^{-}$) and subsequent suppression of thyroid-stimulating hormone by thyroxine therapy (*2*). The prognosis of these 2 tumor types is good when they are limited to the thyroid and cervical lymph nodes but worse when the mediastinum is involved. MTC and most HCCs do not take up $^{131}I^{-}$, and the therapeutic option is therefore surgery, sometimes combined with external radiation therapy. The prognosis related to tumor stage and grade is usually worse than for PC and FC (*2*).

The hormone somatostatin (SS), identified by Kruhlich et al. (*3*), occurs in 2 forms, SS-14 and SS-28. It is normally present in several organs and regulates both endocrine and exocrine secretion (*4–6*). For example, SS suppresses the secretion of growth hormone and insulin. The short biologic half-life of native SS—less than 3 min—limits its use in the treatment of hormone-producing tumors. Octreotide is a potent SS analog (octapeptide) with a receptor-binding site similar to that of SS but with a biologic half-life of approximately 2 h, making it suitable for clinical use (*7*). SS and octreotide bind to specific high-affinity receptors in the cell membrane with 7 transmembrane regions. Five subtypes of SS receptors (*sstr*) have been identified, with each gene located on separate chromosomes. Octreotide has the highest affinity for *sstr2*, lower affinities for *sstr3* and *sstr5*, and the lowest affinity for *sstr1* and *sstr4* (*8*).

Several tumor cell types express *sstr* (*9*). Today, octreotide is used routinely for patients with neuroendocrine tumors for palliation of symptoms by reducing the secretion of various hormones. ^{111}In-labeled octreotide is widely used for scintigraphic visualization of *sstr*-bearing tumors. Octreotide scintigraphy has a high sensitivity (approximately 80%–95%) for several endocrine pancreatic tumors (EPT),

Received Mar. 15, 1999; revision accepted Aug. 5, 1999.

For correspondence or reprints contact: Eva B. Forssell-Aronsson, PhD, Department of Radiation Physics, Sahlgrenska University Hospital, S-413 45 Göteborg, Sweden.

paraganglioma, small-cell lung cancer, and carcinoid tumors (*10–13*). We previously determined ^{111}In concentrations and tumor-to-blood ^{111}In concentration ratios (T/B) for carcinoid tumors, MTC, Hürthle cell neoplasias, and EPT (*14–17*). In general, the T/Bs for carcinoid tumors were high (50–650), and specimens with lower values contained only microscopic tumor growth. The T/Bs varied greatly among different types of EPT. The highest T/B observed was 1500, found in a patient with proinsulinoma and gastrinoma, whereas the lowest ratio was 6, found in a patient with mixed hormone production. For MTC the ratio varied between 2 and 360 (*16*), and only half the tumors could be visualized scintigraphically, a proportion that has also been found in other studies (*16,18–19,20*). Pilot studies showed visualization of some MTC tumors even in the absence of *sstr2*, the receptor with the highest affinity for octreotide (*16*).

Because uptake of ^{111}In-octreotide in normal thyroid tissue is relatively high and few methods are available to localize some thyroid tumor types, such as Hürthle cell neoplasias, we investigated patients with PC, HCC, HCA, and FA using ^{111}In-diethylenetriaminepentaacetic acid (DTPA)-Phe^1-octreotide and compared the findings with data from patients with MTC. The ^{111}In concentration in thyroid tissue samples excised during surgery 1 or several days after injection of ^{111}In-DTPA-Phe^1-octreotide was compared with the *sstr* subtype profiles (by Northern blot analysis) and the relative expression of *sstr2* (by ribonuclease protection assay [RPA]).

MATERIALS AND METHODS

Radiopharmaceutical

DTPA-D-Phe^1-octreotide and ^{111}In-chloride were obtained from Mallinckrodt Medical BV (Petten, The Netherlands). The DTPA-D-Phe^1-octreotide was radiolabeled with ^{111}In according to the instructions of the manufacturer. Instant thin-layer chromatography of the radiopharmaceutical was performed using an ITLC-SG (Gelman Science Inc., Ann Arbor, MI) with sodium citrate (0.1 mol/L, pH of 5) as the mobile phase. The fraction of peptide-bound ^{111}In was more than 98%.

Patients

Forty-six patients with thyroid tumors were included in this study. The thyroid tumors were MTC (n = 23 patients, 5 primary lesions), PC (n = 11 patients, 9 primary lesions), HCC (n = 4 patients, 2 primary lesions), HCA (n = 4 patients, 4 primary lesions), and FA (n = 4 patients, 4 primary lesions). The patients received 180–350 MBq (10 μg) ^{111}In-DTPA-Phe^1-octreotide by intravenous injection. Before and after administration, the activity of the syringe was measured with a well-type ionization chamber (CRC-120; Capintec, Inc., Ramsey, NJ). The study was approved by the local isotope and ethical committees, and the patients gave informed consent. Tumor and thyroid biopsy samples from an additional 20 patients underwent Northern blot analysis.

Tissue Sampling and Examination

The patients underwent surgery 1–15 d after injection of the radiopharmaceutical. Tumor, lymph nodes with or without metastases, and other easily available normal tissue samples such as fat and muscle were excised, and peripheral blood was sampled. The fresh tissue samples were weighed, and the ^{111}In activity was determined. Thereafter, the excised tissues were examined histologically. In 1 MTC patient several tumor-suspect lymph nodes were excised and carefully trimmed from adjacent tissue for detailed analysis of T/Bs and specimen weight and for estimation of relative tumor volume. The MTC cells were immunocytochemically visualized by calcitonin antiserum. The areal density (percentage) of tumor cells in each lymph node was estimated using 3 random sections from each specimen.

^{111}In Activity Measurements

The ^{111}In activity in small tissue samples was measured in a γ counter equipped with a 7.6-cm-diameter) NaI(Tl) well crystal (3-cm hole diameter and 6-cm depth) (Bicron, Newbury, OH) and a single-channel pulse-height analyzer (Elscint Ltd., Haifa, Israel). The calibration factor between the sensitivity of the ionization chamber and the γ counter was determined. Corrections were also made for detector background and radioactive decay.

The ^{111}In activity concentration in tissue, C_{tissue}, was expressed as the fraction of the injected activity, $A_{injected}$, per unit mass of tissue:

$$C_{tissue} = \frac{A_{tissue}/m_{tissue}}{A_{injected}} \times 100,$$

where A_{tissue} is the ^{111}In activity of the tissue sample and m_{tissue} is its mass.

The ^{111}In activity concentration ratios of tissue (Ti) to blood (B) were calculated:

$$Ti/B = \frac{A_{tissue}/m_{tissue}}{A_{blood}/m_{blood}} = \frac{C_{tissue}}{C_{blood}},$$

where A_{blood} is the injected activity per unit mass of blood, m_{blood} is the mass of the blood sample, and C_{blood} is the ^{111}In activity concentration in blood.

Northern Blot Analyses of *sstr1–sstr5* Messenger RNA Expression

Fresh tumor specimens were rapidly frozen in liquid nitrogen. RNA was prepared by acid guanidine thiocyanate-phenol-chloroform extraction. Samples of total RNA (20 μg) were denatured with heat and electrophoresed in 1% agarose gel with 2.2 mol/L formaldehyde, 1 mmol/L ethylenediaminetetraacetic acid, 5 mmol/L sodium acetate, and 20 mmol/L morpholine propane sulfonic acid (pH of 7.0) as a running buffer. RNA was transferred to positively charged nylon membranes (Boehringer, Mannheim, Germany) using a vacuum transfer system (Hybaid, Middlesex, UK) and cross-linked to the membrane by ultraviolet light (Stratalinker; Stratagene, La Jolla, CA). Membranes were hybridized in rotating flasks (Hybaid) at 65°C using the following ^{32}P-labeled antisense RNA probes: a 1.126-bp PCR fragment of the human *sstr1* gene corresponding to nucleotides 352–1478 (*21*), a 1.7-kb Bam HI/Hind III cDNA fragment of the human *sstr2* gene (*21*), a 1.9-kb Nco/Hind III cDNA fragment of the human *sstr3* gene (*22*), a 2.0-kb Nae I/Xbal cDNA fragment of the human *sstr4* gene (*23*), a 1.6-kb Eco R1/Sal III cDNA fragment of the human *sstr5* gene (*24*), and a 982-bp fragment of the human G3PDH gene.

Specific labeling was detected after 3–6 d of exposure on an imaging plate, followed by reading in a phosphor imager (Molecular Dynamics, Sunnyvale, CA).

RPA Analysis of *sstr2*

Fresh tumor specimens were carefully trimmed of residual normal tissue, rapidly frozen in liquid nitrogen, and stored at −80°C until extraction of RNA. Total RNA was prepared by acid guanidinium thiocyanate-phenol-chloroform extraction (*25*). RNA concentrations were estimated by ultraviolet spectrophotometry at 260 nm. Aliquots of the RNA samples were electrophoresed in 1% agarose gel stained with ethidium bromide to confirm the integrity of the isolated RNA.

To quantify the expression of human *sstr2* in tumor biopsies, an RPA was developed.

Probes. pGEM-3Z containing a 1.7-kb human *sstr2* cDNA insert (M81830) was used. Initially, 3 PCR fragments were cloned from the recombinant plasmid corresponding to nucleotides 777–1116 (2F1), 957–1225 (2F2), and 1300–1669 (2F3). The clone 2F2 was chosen as the probe for the RPA assay because of high sensitivity and linearity. As an internal control, a 316-bp reduced human glyceraldehyde-phosphate dehydrogenase (hGAPDH) antisense probe template (catalog no. 7430; Ambion Inc., Austin, TX) was used.

Probe Synthesis. Linearized 2F2 plasmid and an hGAPDH template were used to prepare ^{32}P-labeled antisense probes using T3 RNA polymerase, T7 RNA polymerase, and ^{32}P-α-UTP (Amersham Pharmacia, Freiburg, Germany).

Hybridization and Electrophoresis. For hybridization of RNA, an RPA II kit (Ambion) was used. A cocktail of 40,000–50,000 cpm h*sstr2* antisense probe and 10,000–15,000 cpm hGAPDH antisense probe, as an internal control, was mixed with 5–30 μg total RNA, prepared from tumor biopsies, and was precipitated with ethanol for 1 h. The RNA precipitate was resuspended in 20 μL hybridization solution (Ambion), denatured for 3 min at 93°C, and hybridized at 43°C for 15–18 h. To the hybridization solution was added a 200-μL mixture of RNase A and RNase T1 at a 1:10,000 dilution. Incubation at 37°C for 30 min followed. The reaction was stopped by adding 300 μL RNase inactivation–precipitation mixture. After ethanol precipitation at −20°C for 1 h, the pellet was washed in ethanol and resuspended in 6 μL loading buffer. Samples were denatured at 93°C and electrophoresed on 6% polyacrylamide-urea gel (EC68655; Novex, San Diego, CA). The gel was run at 180 V for 1.5 h.

Quantification. Protected RNA fragments were read in the phosphor imager after 12–20 h exposure on an imaging plate. The density of the RNA bands was measured using the ImageQuant program (Molecular Dynamics). To adjust for variations in the amount of RNA loaded, ratios of h*sstr2* to hGAPDH were calculated. The ratios were compared with those of RNA extracts from the h*sstr2*-expressing cell line NCI-H69 (American Type Culture Collection, Rockville, MD), which were included in each assay. Ratios exceeding 0.2–0.4 (variation caused by individual assay conditions) were regarded as significant. Detection of *sstr2* and GAPDH hybrids was linear over the interval of 0.5–20 μg total RNA isolated from NCI-H69. All samples were within this interval.

RESULTS

T/B

Table 1 shows the T/Bs. The highest T/B values were 360 for MTC, 190 for FA, 140 for HCA, 67 for HCC, and 70 for PC. No obvious change was seen with time after injection.

TABLE 1
T/Bs for Thyroid Tumor Tissues After Injection of ^{111}In-Labeled Octreotide

Time after injection (d)	MTC	PC	HCC	HCA	FA
1	4–39 (10)	7–66 (2)*	11–380 (6)		23–27 (2)
	3–39 (8)	3–20 (6)*			
	3–9 (3)	21 (1)			
2	14 (1)	41 (1)			
	4–33 (6)*				
	22–47 (4)				
	14–69 (4)†				
	104 (1)†				
3		2–15 (12)			
5	15–18 (4)	10–54 (3)*		35–45 (2)*	190 (1)
	11–24 (2)	2–10 (6)		76 (1)†	64 (1)*
	3–43 (2)	29 (1)*		68–140 (2)	
	36 (1)	16–52 (2)		37 (1)	
	4–13 (3)*	61 (1)			
	3–240 (9)†				
	17–140 (5)†				
	30–47 (3)				
	39–54 (2)†				
	26–53 (4)				
6	2–32 (16)	55 (1)	11–53 (2)†		77 (1)
7	3–360 (5)†		18–55 (2)		
	6–14 (7)				
	27–34 (2)				
8	8–75 (7)†				
15			38–67 (2)		

*Biopsies without expression of *sstr2* at Northern blot analysis.
†Biopsies with expression of *sstr2* at Northern blot analysis.
Each line represents data from 1 patient. Numbers in parentheses indicate number of tissue samples collected from patient.

MTC tumors were studied in 23 different patients 1–8 d after injection. High T/Bs (>50) were observed after 2, 5, 7, and 8 d.

Ratios of Nontumor Thyroid Tissue to Blood

Table 2 shows the ratios of nontumor thyroid tissue to blood. Thyroid tissue samples were obtained from the contralateral lobe in patients subjected to total thyroidectomy. The histologic examination showed normal thyroid tissue in 9 patients, colloid goiter in 5 patients, and thyroiditis in 5 patients. The ratios of normal thyroid tissue to blood were 7–18 when measured 1–8 d after injection. The ratios of colloid goiter to blood were somewhat higher (8–48), and the ratios of thyroiditis to blood were more variable (7–120).

Relationship Between T/B and Tumor Volume

The relationship between T/B and tumor volume was examined in 1 patient with 5 lymph node metastases from MTC. No correlation was found between the T/B and the weight of the excised tumor specimens (Fig. 1A). Similar data were observed for 12 patients with various thyroid tumor types. However, when T/B was plotted against the

TABLE 2
Ratios of Nontumor Thyroid Tissue to Blood After Injection of ^{111}In-Labeled Octreotide

Time after injection (d)	Normal thyroid	Nodular goiter	Thyroiditis
1		8–10 (2)	
		30–48 (4)	
			120 (1)
			25 (1)
			7 (1)
5		26–35 (4)	
			26 (1)
	18 (1)		18–71 (2)
	10 (2)		
	9 (1)		
		27 (1)	
		14 (1)	
	7 (1)		
	16 (1)		
	17 (1)		
	11 (1)		
6	10 (1)		
8	8–9 (2)		

Each line represents data from 1 patient. Numbers in parentheses indicate number of tissue samples collected from patient. Tissues were obtained from non–tumor-bearing lobe in patients subjected to total thyroidectomy.

fraction of immunoreactive tumor cells (from morphometric analyses), the relationship was linear ($r = 0.93$, $P < 0.05$) (Fig. 1B).

Northern Blot Analyses

Table 3 shows the receptor subtype expression in biopsied tumor tissue from some of the study patients and additional patients with the same histopathologic diagnosis. In all tumor types investigated, *sstr1*, *sstr3*, *sstr4*, and *sstr5* were regularly expressed. *sstr2* was expressed in most MTC tumors but was not detected in any FA or PC tumors. In HC neoplasia, the expression of *sstr2* was irregular. The 5 patients who had AC (T/Bs not determined) all lacked *sstr2* expression.

RPA Analyses

Table 4 compares the relative *sstr2* expression, analyzed by RPA, and the T/B of biopsied primary tumors (n = 14). The *sstr* subtype expression of several tumors was also analyzed using the Northern blot method. The T/Bs for all tumors ranged from 20 to 190, and the corresponding relative RPA values ranged from 0.3 to 1.5. Five of 9 tumors studied lacked expression of *sstr2* on Northern blot analysis. When T/Bs for all tumor types in this limited material were compared with the corresponding RPA values for *sstr2*, no correlation was seen.

DISCUSSION

Initial observations on radiopharmaceutical accumulation of octreotide in the normal thyroid gland were corroborated by in vitro findings on SS actions, e.g., inhibition of adenyl cyclase activation by thyroid-stimulating hormone (*26*). In thyroid cancer cell lines, SS inhibited cell growth and was a ligand binding to the cell membranes (*27–29*). Tenenbaum et al. (*30*) studied 14 patients with differentiated thyroid carcinoma by means of octreotide scintigraphy and found a variable capacity to image distant metastases. In a subsequent study, Postema et al. (*31*) investigated 21 nonmedullary thyroid tumors by octreotide scintigraphy with specific uptakes in all patients with primary tumors. No obvious difference in sensitivity was observed between follicular and papillary tumor types. Visualization of such tumors is corroborated by our relatively high T/Bs versus normal thyroid tissue despite the lack of *sstr2* at Northern blot analysis.

In our own scintigraphic studies of MTC and Hürthle cell tumors (*16*) we could visualize half the MTC tumors, in accordance with the findings of several other investigators, such as Baudin et al. (*19*). In 10 consecutive patients with Hürthle cell lesions, all surgically identified tumors were visualized (*17*). These 2 studies indicate that thyroid tumors that do not concentrate radioiodine, such as MTC and Hürthle cell lesions, can be visualized through their expression of *sstr*. Octreotide scintigraphy may therefore complement radioiodine scintigraphy in the diagnosis of residual neck tumors and distant metastases after previous thyroidec-

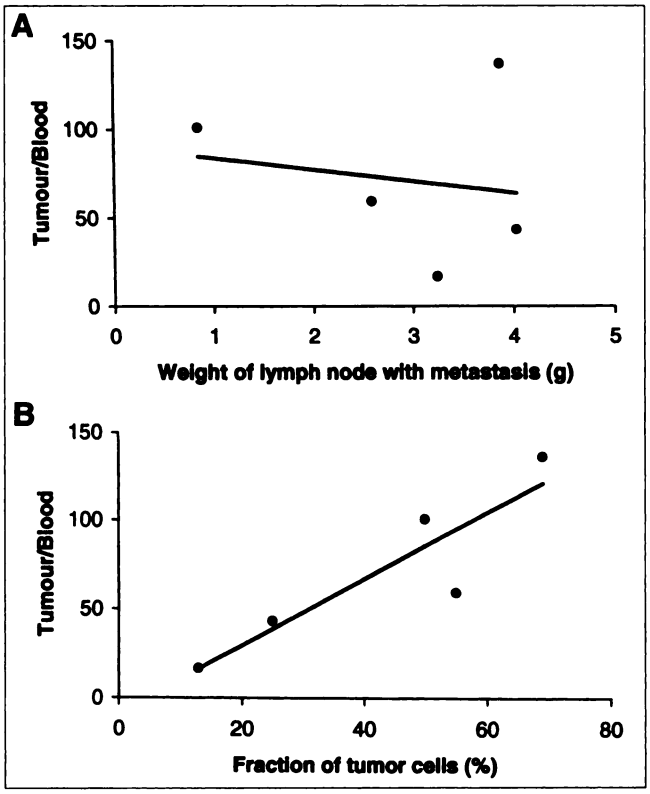

FIGURE 1. Results from 1 patient with MTC. T/B is given versus weight of excised regional lymph node specimen (containing tumor metastases) (A) and relative fraction of immunoreactive tumor cells (from morphometric analyses) (B).

tomy. Basic knowledge of *sstr* subtype profiles and of binding and internalization of octreotide-carried radionuclides is also important in evaluating the potential usefulness of receptor-mediated radiotherapy. Furthermore, some investigators have proposed that the functional differentiation of MTC tumors may relate to the expression of *sstr* and may serve as a potential indicator of prognosis (*16,18,30,32*).

Uptake of radiopharmaceuticals into tumors is usually presented as the ratios between the radionuclide concentration in tumor tissue and in relevant normal tissues. T/B is widely used because blood is easily available and is a relevant parameter for intravenously injected radiopharmaceuticals. We previously found wide variations in T/B for several neuroendocrine tumors, with high values for carcinoid tumors (27–650) and sometimes very high values for EPT (910–1500) (*14,15*). In the present series of thyroid tumors, somewhat lower values were generally seen. The highest T/Bs were in MTC tumors and individual patients with FA and Hürthle cell lesions. This finding may reflect the fact that MTC tumors and Hürthle cell neoplasia were the only tumor types in our series that showed expression of the high-affinity *sstr2* in Northern blot analysis. With the assumption that the individually highest T/B better represents true tumor cell binding (Fig. 1), we analyzed these T/Bs for all thyroid tumors, which were also studied by Northern blot analysis (Table 1). The tumors with *sstr2* expression had significantly ($P < 0.03$) higher T/Bs (150 ± 35 [mean ± SD]) than those lacking such expression (39 ± 7). Our findings partly contrast with recent findings of Mato et al. (*33*), who used reverse transcriptase (RT)-PCR for MTC from 14 patients. Mato et al. found the expression of more than 1 *sstr* subtype in 10 patients. Most frequently, *sstr2* was expressed, whereas *sstr4* was not expressed. Part of the discrepancy in T/B between carcinoids and, for example, MTC may be caused by much lower tumor volumes in MTC. Many MTC cases in this study were early recurrences diagnosed by sensitive biochemical methods (pentagastrin tests and serum calcitonin determinations). Other factors may be different proportions of tumor cells in individual biopsies (Fig. 1) and possible heterogeneity of *sstr* expression between primary tumors and metastases. These factors may also explain the intra- and interindividual variations seen (Table 1). In some studies using radiolabeled monoclonal antibodies and subcutaneously implanted tumors, T/B decreased with increasing tumor size (*34*). This finding was not the case in our patients with neuroendocrine tumors (*14*) or in the 13 patients with thyroid tumors studied here (Fig. 1A).

The ratio of nontumor thyroid tissue to blood was in some cases much higher for thyroiditis (maximum value, 120) and for colloid goiter (maximum value, 48) than for normal

TABLE 3
sstr Subtypes in Tissues Studied by Northern Blot Analysis

Thyroid tissue	*sstr1*	*sstr2*	*sstr3*	*sstr4*	*sstr5*
Tumor type					
MTC (n = 9)	+	0	++	++	++
	++	+	++	++	++
	++	+	++	++	++
	+	ND	0	++	++
	+	+	++	++	++
	+	0	++	++	++
	++	+	++	++	++
	++	ND	++	++	++
	++	++	++	++	++
PC (n = 9)	+	0	++	++	++
	++	0	++	++	++
	++	0	++	++	++
	++	0	++	++	++
	+	ND	++	++	++
	+	0	++	++	++
	+	0	++	++	+
	++	0	++	++	++
	++	0	++	++	++
HCC (n = 2)	+	++	++	++	++
	++	0	++	++	++
HCA (n = 4)	++	+	++	++	++
	++	0	++	++	++
	+	0	++	++	++
	ND	ND	++	++	++
FA (n = 8)	++	0	++	++	++
	++	0	++	++	++
	++	ND	++	++	++
	++	0	++	++	++
	++	0	++	++	++
	++	0	++	++	++
	++	0	++	++	++
	++	0	++	ND	++
AC (n = 5)	+	0	++	++	++
	+	0	++	++	++
	++	0	++	++	++
	++	0	++	++	++
	++	0	++	++	++
Nontumor type					
Normal	+	0	++	++	++
	+	0	++	++	++
Thyroiditis	+	0	++	++	++
	ND	ND	++	ND	ND

+ = twice the background; 0 = no signal; ++ = more than twice the background; ND = not done.
One tumor sample per patient.

TABLE 4
T/Bs and Expression of *sstr2* in Thyroid Tumors

Tumor type	Presence of *sstr2**	Mean T/B (range)	Mean *sstr2*† (range)
MTC (n = 4)	2/2	58 (39–94)	0.78 (0.61–0.94)
PC (n = 3)	0/3	39 (20–66)	0.91 (0.54–1.5)
HCC (n = 1)	1/1	53	0.98
HCA (n = 3)	1/2	52 (37–76)	0.52 (0.30–0.74)
FA (n = 3)	0/1	92 (25–190)	0.83 (0.52–1.1)

*Studied by Northern blot analysis.
†Studied by RPA.
One tumor sample per patient.

thyroid tissue (range, 7–18) (Table 2). The Northern blot analyses of normal thyroid tissue and inflamed thyroid tissue showed expression of all *sstr* subtypes except *sstr2*; i.e., the expression was similar to that observed for most of the thyroid tumors (Table 3). In a study by Ain et al. (*29*), normal thyroid tissue showed expression of *sstr3* and *sstr5*, weak expression of *sstr1* and *sstr2*, and no expression of *sstr4* when examined using RT-PCR. A previously reported relatively high uptake of ^{111}In in benign thyroid conditions (endemic colloid goiter, thyroid autonomy, and Graves' disease) was confirmed by this study (*35,36*). This confirmation means that the relatively high uptake in benign thyroid conditions may limit the role of ^{111}In-octreotide for diagnosis of primary tumors but not for diagnosis of distant metastases (*16,17*).

MTC cells were stained immunocytochemically with a calcitonin antiserum, and the relative proportion of tumor cells was estimated morphometrically. The results showed that T/B was linearly correlative with the proportion of tumor cells in the biopsy but was not correlative with the weight of the metastatic lymph node (Fig. 1). This finding indicates that ^{111}In-octreotide binding to tumor cells is much higher than the degree of binding represented by T/Bs in whole-tumor specimens (Table 1); i.e., some patients with low T/Bs for whole-tumor specimens may have very high T/Bs for tumor cells.

For technical reasons, RPA analysis of the *sstr2* mRNA concentration and T/B could not be performed on identical tissue samples. Primary tumors were divided into 2 parts, which were analyzed separately using the 2 methods. Nine of 14 tumors analyzed for *sstr2* expression by RPA and T/Bs also underwent Northern blot analysis of *sstr* subtypes. The negativity of 5 of these 9 tumors for *sstr2* expression reflects the much higher sensitivity of the RPA method for receptor detection. In this study, all tumors had values above the significance level in the RPA assay system. The apparent discrepancy between RPA and T/Bs may be because T/Bs largely reflect octreotide binding to *sstr* subtypes other than *sstr2*. This possibility may be the case for thyroid tumors, in which expression of *sstr2* is frequently low. In our pilot study (*16*) and a recent study by Bernà et al. (*37*), individual MTC tumors, visualized by octreotide scintigraphy, were actually devoid of *sstr2* expression when studied by Northern blot analysis or RT-PCR. Another explanation may be heterogeneity in the expression of *sstr* within each tumor.

With our present knowledge, use of radiolabeled octreotide for therapy of some EPTs and carcinoids may be possible. Using endocrine tumor cell lines, [^{90}Y-DOTA^0, Tyr^3]octreotide was internalized in higher amounts than were the^{111}In-labeled octreotide variants (*38*). One clearly needs an octreotide labeled with radionuclides that are more suitable for therapy than are ^{111}In and ^{90}Y and have favorable subcellular distribution and microdosimetry in tumors and normal tissues. The observed variation in T/B (gross tumor specimens) for metastases of thyroid carcinoma in an individual patient does not preclude radiation therapy, because a high T/B was found in true tumor tissue estimated morphometrically. Octreotide-borne radionuclides whose emitted particles have a short range should therefore be considered as first candidates. Theoretically, *sstr* expression and uptake in endocrine tumors may be upregulated by hormonal manipulation (*39*). Because of large individual variations in uptake in normal tissues, individualized dose planning will be necessary. Elevated T/Bs in cases of thyroiditis is a minor problem, because radiation therapy will be the first type of therapy instituted after removal of the thyroid. Characterization of *sstr* subtype expression in thyroid carcinoma may permit targeting of specific analogs and inhibit proliferation of both differentiated and anaplastic tumors, as has been shown in vitro (*29*). Such subtype-specific analogs, if suitably radiolabeled, will facilitate individualized *sstr*-mediated radiation therapy.

CONCLUSION

The high T/Bs observed in MTC tumors and in follicular and Hürthle cell lesions can easily be explained by their expression of the high-affinity *sstr2*. However, despite the lack of *sstr2* expression of certain thyroid tumors at Northern blot analysis, relatively high T/Bs were observed. This finding likely reflects substantial binding of ^{111}In-DTPA-Phe^1-octreotide to other subtypes of *sstr*. In morphometric analyses, T/B correlated linearly with the fraction of tumor involvement in lymph node metastases, strongly indicating higher binding and uptake of radionuclide in tumor cells than in surrounding normal tissue. The T/B of an excised tumor-affected lymph node is thus an underestimation of the true T/B, a fact that favors the possibility of future *sstr*-borne radiation therapy for certain thyroid tumors.

ACKNOWLEDGMENTS

The authors thank Lena William-Olsson for expert technical assistance. This work was supported by grants from the Swedish National Cancer Society (2998, 3427), the Swedish Medical Research Council (5220), the Landmann Foundation, and the IB & A Lundberg Research Foundation, Göteborg, Sweden. The *sstr2* and *sstr3* probes were gifts from Dr. Graeme I. Bell, University of Chicago, Chicago, IL. The *sstr4* probe was a gift from Dr. Friedrich Raulf, Sandoz, Basel, Switzerland. The *sstr5* probe was a gift from Susumo Seino, Chiba University School of Medicine, Japan.

REFERENCES

1. Rosai J, Carcangiu ML, DeLellis RA. Tumors of the thyroid gland. In: *Atlas of Tumor Pathology.* Ser. 3, fasc. 5. Washington, DC: Armed Forces Institute of Pathology; 1992.
2. Schlumberger MJ. Papillary and follicular thyroid carcinoma. *N Engl J Med.* 1998;338:297–306.
3. Kruhlich L, Dhariwal A, McCann S. Stimulatory and inhibitory effects of purified hypothalamic extracts on growth hormone release from rat pituitary in vitro. *Endocrinology.* 1968;83:783–790.
4. Reichlin S. Somatostatin. Part 1. *N Engl J Med.* 1983;309:1495–1501.
5. Reichlin S. Somatostatin. Part 2. *N Engl J Med.* 1983;309:1556–1563.
6. Shulkes A. Somatostatin: physiology and clinical applications. *Baillieres Clin Endocrinol Metab.* 1994;8:215–236.

7. Bauer W Briner U, Doepfner W, et al. SMS-201–995: a very potent and selective octapeptide analogue of somatostatin with prolonged action. *Life Sci.* 1982;31: 1133–1140.
8. Bruns C, Weckbecker G, Raulf F, et al. Molecular pharmacology of somatostatin-receptor subtypes. *Ann N Y Acad Sci.* 1994;733:138–146.
9. Reubi J-C, Krenning E, Lamberts S, et al. Somatostatin receptors in malignant tissue. *J Steroid Biochem Mol Biol.* 1990;37:1073–1077.
10. Krenning EP, Kwekkeboom DJ, Bakker WH, et al. Somatostatin receptor scintigraphy with (^{111}In-DTPA-D-Phe^1)- and (^{123}I-Tyr^3)-octreotide: the Rotterdam experience with more than 1000 patients. *Eur J Nucl Med.* 1993;20:716–731.
11. Ahlman H, Wängberg B, Tisell LE, et al. Clinical efficacy of octreotide scintigraphy in patients with midgut carcinoid tumors and evaluation of intraoperative scintillation detection. *Br J Surg.* 1994;81:1144–1149.
12. Jamar F, Fiasse R, Leners N, Pauwels S. Somatostatin receptor imaging with indium-111-pentetreotide in gastroenteropancreatic neuroendocrine tumors: safety, efficacy and impact on patient management. *J Nucl Med.* 1995;36:542–549.
13. Reisinger I, Bohuslavitzki KH, Brenner W, et al. Somatostatin receptor scintigraphy in small-cell lung cancer: results of a multicenter study. *J Nucl Med.* 1998;39:224–227.
14. Forssell-Aronsson E, Fjälling M, Nilsson O, et al. Indium-111-activity concentration in tissue samples after intravenous injection of indium-111-DTPA-D-Phe-1-octreotide. *J Nucl Med.* 1995;36:7–12.
15. Wängberg B, Nilsson O, Johansson V, et al. Somatostatin receptors in the diagnosis and therapy of neuroendocrine tumors. *The Oncologist.* 1997;2:50–58.
16. Tisell LE, Ahlman H, Wängberg B, et al. Somatostatin receptor scintigraphy in medullary thyroid carcinoma. *Br J Surg.* 1997;84:543–547.
17. Tisell LE, Ahlman H, Wängberg B, et al. Expression of somatostatin receptors in oncocytic (Hürthle cell) neoplasia of the thyroid. *Br J Cancer.* 1999;79:1579–1582.
18. Kwekkeboom DJ, Reubi JC, Lamberts SWJ, et al. *In vivo* somatostatin receptor imaging in medullary thyroid carcinoma. *J Clin Endocrinol Metab.* 1993;76:1403–1417.
19. Baudin E, Lumbroso J, Schlumberger M, et al. Comparison of octreotide scintigraphy and conventional imaging in medullary thyroid carcinoma. *J Nucl Med.* 1996;37:912–916.
20. Behr TM, Gratz S, Markus PM, et al. Enhanced bilateral somatostatin receptor expression in mediastinal lymph nodes ("chimney sign") in occult metastatic medullary thyroid cancer: a typical site of tumor manifestation? *Eur J Nucl Med.* 1997;24:184–191.
21. Yamada Y, Post SR, Wang K, Tager HS, Bell GI, Seino S. Cloning and functional characterization of a family of human and mouse somatostatin receptors expressed in brain, gastrointestinal tract and kidney. *Proc Natl Acad Sci USA.* 1992;89:251–255.
22. Yamada Y, Reisine T, Law SF, et al. Somatostatin receptors, an expanding gene family: clonal and functional characterization of human *SSTR3*, a protein coupled to adenyl cyclase. *Mol Endocrinol.* 1992;6:2136–2142.
23. Rohrer L, Raulf F, Bruns C, Buettner R, Hofstaedter F, Schule R. Cloning and characterization of a fourth somatostatin receptor. *Proc Natl Acad Sci USA.* 1993;90:4196–4200.
24. Yamada Y, Kagimoto S, Kubota A, et al. Cloning, functional expression and pharmacological characterization of a fourth (*SSTR4*) and a fifth (*SSTR5*) human somatostatin receptor subtype. *Biochem Biophys Res Commun.* 1993;195:844–852.
25. Chomczynski P, Sacchi N. Single-step method of RNA isolation by acid guanidinium thiocyanate-phenol-chloroform extraction. *Anal Biochem.* 1987;162: 156–159.
26. Siperstein AE, Kenneth EL, Gum ET, Clark OH. Effect of somatostatin on adenylate cyclase activity in normal neoplastic thyroid tissue. *World J Surg.* 1992;16:555–561.
27. Hoelting T, Zielke A, Siperstein AE, et al. Tamoxifen and octreotide inhibit growth invasion and protease activity in papillary and follicular thyroid cancer [abstract]. *J Endocrinol Invest.* 1993;16:33.
28. Ain KB, Taylor KD. Somatostatin analogs affect proliferation of human thyroid carcinoma cell lines *in vitro*. *J Clin Endocrinol Metab.* 1994;78:1097–1102.
29. Ain KB, Taylor KD, Tofiq S, Venkataraman G. Somatostatin receptor subtype expression in human thyroid and thyroid carcinoma cell lines. *J Clin Endocrinol Metab.* 1997;82:1857–1862.
30. Tenenbaum F, Lumbroso J, Schlumberger M, Caillou B, Fragu P, Parmentier C. Radiolabeled somatostatin analog scintigraphy in differentiated thyroid carcinoma. *J Nucl Med.* 1995;36:807–810.
31. Postema PTE, de Herder WW, Reubi JC, et al. Somatostatin receptor scintigraphy in non-medullary thyroid cancer. *Digestion.* 1996;57:36–37.
32. Adams S, Baum RP, Hertel A, Schumm-Draeger PM, Usadel K-H. Comparison of metabolic and receptor imaging in recurrent medullary thyroid carcinoma with histopathological findings. *Eur J Nucl Med.* 1998;25:1277–1283.
33. Mato E, Matias-Guiu X, Chico A, et al. Somatostatin and somatostatin receptor subtype gene expression in medullary thyroid carcinoma. *J Clin Endocrinol Metab.* 1998;83:2417–2420.
34. Williams LE, Duda RB, Proffitt RT, et al. Tumor uptake as a function of tumor mass: a mathematical model. *J Nucl Med.* 1988;29:103–109.
35. Becker W, Schrell U, Buchfelder M, et al. Somatostatin receptor expression in the thyroid demonstrated with ^{111}In-octreotide scintigraphy. *J Nucl Med.* 1995;34:100–103.
36. Garancini S, La Rosa S, De Palma D, Uccella S, Golonia F. Uptake of In-111 pentetreotide by normally functioning nodular goiters. *Clin Nucl Med.* 1997;22: 625–627.
37. Bernà L, Chico A, Matías-Guiu X, et al. Use of somatostatin analogue scintigraphy in the localization of recurrent medullary thyroid carcinoma. *Eur J Nucl Med.* 1998;25:1482–1488.
38. de Jong M, Bernard BF, de Bruin E, et al. Internalization of radiolabeled [DTPA^0]octreotide and [DOTA^0, Tyr^3]octreotide: peptides for somatostatin receptor-targeted scintigraphy and radionuclide therapy. *Nucl Med Commun.* 1998;19:283–288.
39. Visser-Wisselaar HA, Van Uffelen CJ, Van Koetsveld PM, et al. 17-beta-estradiol-dependent regulation of somatostatin receptor subtype expression in the 7315b prolactin secreting rat pituitary tumor in vitro and in vivo. *Endocrinology.* 1997;138:1180–1189.